Proceedings of the

Advanced Architectures in Photonics

September 21−24, 2014
Prague, Czech Republic

Volume 1

Editors

Jiri Orava

University of Cambridge
Department of Materials Science and Metallurgy
27 Charles Babbage Road
CB3 0FS Cambridge
United Kingdom

Tohoku University
WPI-Advanced Institute for Materials Research
(WPI-AIMR)
2-1-1 Katahira, Aoba-ku
980-8577 Sendai
Japan

Tomas Kohoutek

Involved Ltd.
Siroka 1
537 01 Chrudim
Czech Republic

CONTENTS

Innovative nanoimprint lithography

S. Matsui,[1,2,*] H. Hiroshima,[2,3] Y. Hirai,[2,4] and M. Nakagawa[1,5]

[1] *Laboratory of Advanced Science and Technology for Industry, University of Hyogo, 3-1-2 Koto, Kamigori, Ako, Hyogo 678-1201, Japan*
[2] *JST-CREST, 5 Sambancho, Chiyoda, Tokyo 102-0075, Japan*
[3] *Research Center for Ubiquitous MEMS and Micro Engineering, National Institute of Advanced Science and Technology, 1-2-1 Namiki, Tsukuba 305-8564, Japan*
[4] *Graduate School of Engineering, Osaka Prefecture University, 1-1 Gakuen-cho, Nakaku, Sakai, Osaka, 599-8531, Japan*
[5] *Institute of Multidisciplinary Research for Advanced Materials, Tohoku University, 2-1-1 Katahira, Aoba-ku, Sendai 980-8577, Japan*

*Electronic mail: matsui@lasti.u-hyogo.ac.jp

The effectiveness of condensable gas, used as ambience, in UV nanoimprint lithography has been demonstrated. Bubble defect problem, which is inherent in UV nanoimprint under non vacuum ambience, can be solved by PFP condensable gas. UV nanoimprint lithography using PFP was validated for 45 nm pattern fabrication under thin residual layer conditions, which are required for UV nanoimprint used as UV nanoimprint lithography. PFP reduces the viscosity and demolding force of UV curable resins. These properties are helpful in increasing the throughput and reliability of UV nanoimprint. PFP occasionally produces large shrinkages, and degrades pattern quality depending on UV curable resin. These drawbacks can be mitigated by selecting UV curable monomers with a low PFP absorption. In the end, we have demonstrated the satisfied LER and LWR values requested in 22 nm node NAND flash memories and 20,000 repeated imprints with a single mold by UV nanoimprint using PFP.

Nanoimprint [1] has been recognized as a promising nanofabrication technique since 1995, when Prof. Chou demonstrated 25 nm wide patterns in polymethylmethacrylate. The nanoimprint was based on thermoplastic property of polymers. Nanoimprint processes are carried out at a raised temperature in order to soften the target polymers and hence called thermal nanoimprint [1]. Soon after the demonstration of thermal nanoimprint, UV (ultraviolet) nanoimprint using photo-curable resins was developed [2]. Photo-curable liquid resins for UV nanoimprint are molded using transparent molds typically made of quartz, and cured by UV irradiation through the molds at room temperature. UV nanoimprint does not require any heating/cooling cycles or high imprint pressures because of the low viscosities of UV curable resin used in the process. The viscosities of UV curable resins are several orders of magnitude lower than those of polymers used during the processing at a raised temperature in thermal nanoimprint. Therefore, UV nanoimprint is considered as a promising candidate of next generation lithography with high resolution and low cost. UV nanoimprint is carried out at a constant temperature and requires very low pressing pressure. Both conditions are desirable for precise patterning required in lithography. However, when UV nanoimprint is carried out in air, the low pressing pressure causes formation of air bubble defects [3] which are not encountered in thermal nanoimprint that employs a high pressing pressure. Application of vacuum ambience solves the problem [4] but not without sacrificing the cost-effectiveness of nanoimprint. Therefore, the air bubble defects should be addressed under non-vacuum conditions. Use of resin droplets in helium ambience is proposed as a viable solution in S-FIL [5] (later renamed as J-FIL), where resin droplets merge each other [6] preventing helium from being trapped during molding process; although small amounts of trapped helium bubbles left behind are dissolved in the photo-curable resin. This method works well but it is not compatible to uniformly pre-coated UV curable resins prepared by spin-coating. To overcome the above problem, we proposed a unique UV nanoimprint method using condensable gas for bubble elimination, which we call "Hiroshima method" [3, 7–9]. We carried out the JST-CREST project "Research and Development on Process Science and CD Control in High-Throughput UV Nanoimprint" in 2008-2014. One of the adopted core technology is using condensable gas which allows the application of spin-coating to achieve high throughput. To realize the high-performance UV-NIL process, understanding the process physics and chemistry in UV-NIL is essential to optimize process conditions and material characteristics. In this paper, we describe the achievements using the new processes, simulations, and materials developed through the JST-CREST project.

The principle of bubble elimination in UV nanoimprint using condensable gas is illustrated in Fig. 1(a) [3]. The key feature of the gas is condensation by a pressure slightly higher than the atmospheric pressure. A gas 1,1,1,3,3-Pentafluoropropane ($CHF_2CH_2CF_3$, HFC-245fa, CAS No. 460-73-1; PFP) is the most
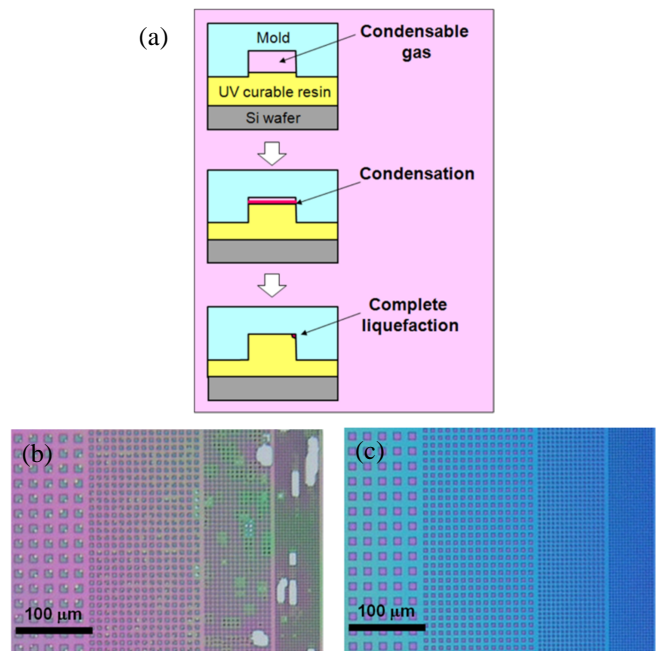
Figure 1. (a) Schematic principle of bubble elimination by condensable gas. UV nanoimprint (a) without and (b) with PFP introduction.

promising candidate since it has properties of non-flammable, safe, low cost, zero ozone depletion potential and so on [7].

At the beginning of contact between the mold and UV curable resin, an isolated recess of a mold traps environmental gas in the imprinting space. The trapped gas is compressed by the mold and the volume of gas decreases. The volume of the trapped gas would be inversely proportional to the gas pressure, however, the relationship breaks down when an increasing pressure reaches to the saturated vapour pressure of the trapped gas (e.g. 0.15 MPa for PFP). The pressure remains constant with decreasing the volume of the trapped gas by condensation (liquefaction). Then, the trapped gas is completely liquefied. In the case of PFP, the liquid volume turns out to be 1/200 of the gas volume. One could suspect that the small liquid PFP droplets would create bubble defects, but, no such defects have been observed so far. We think that PFP remains as a thin layer between the mold and UV curable resin or dissolves in UV curable resin.

UV nanoimprint at an imprint pressure of 0.5 MPa was carried out in air ambience onto a 900-nm-thick UV curable resin (PAK-01, Toyo Gosei) using a quartz mold (NIM-PH350, NTT-AT) containing 350 nm to 10µm wide patterns with a depth of 350 nm. Figure 1(b) shows
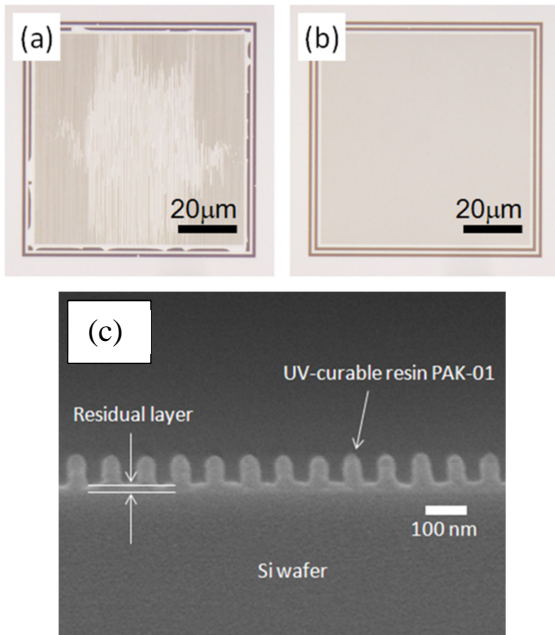
Figure 2. Optical microscope images of UV nanoimprint (a) in air and (b) in PFP. The 45 nm line and space patterns are fabricated in the region fringed by 1µm lines and spaces. (c) Cross-sectional SEM images of 45 nm line and space patterns fabricated by UV nanoimprint in PFP under thin residual layer conditions.

Table I. Simulation parameters.

Viscosity of resist, η (mPa s)	50
Resist surface tension (N m^{-1})	0.0275
Contact angle between resist and template, θ (deg)	60
Imprint pressure for backside of the template, P_T (MPa)	0.1
Critical pressure of condensable gas, P_V (MPa)	0.15
Line width, W (nm)	140
Space, s (nm)	280
Pattern height, d (nm)	140
Initial thickness of the resist, h_0 (nm)	100
Density of the mold, ρ_T (kg m^{-3})	2500
Density of the resist, ρ_R (kg m^{-3})	1140

fabricated patterns by UV nanoimprint without PFP introduction, or in air [7]. Many bubble defects were generated. Trapping of air in isolated recesses (e.g. 10µm squares in Fig. 1(b)) of a mold is quite likely to occur, which shows that the bubble defect problem is inherent to UV nanoimprint in air. Figure 1(c) shows cured resin patterns obtained by UV nanoimprint with 2500 sccm flow of PFP [7] under the aforementioned imprint conditions except for the PFP introduction. The patterns show no bubble defects in contrast to the results obtained in air. The results clearly show the effectiveness of PFP for UV nanoimprint.

When a very thin UV curable resin film is used in UV nanoimprint, bubble elimination is hardly realizable by absorption of the trapped gas into the resin, due to a decrease in the ratio of solvent volume (i.e. UV curable resin volume) to the trapped gas volume. The applicability of UV nanoimprint using PFP to about 20-nm-thick residual layer conditions was examined. Such a thin residual layer is highly-desirable for UV nanoimprint lithography. Figure 2(a) and 2(b) shows optical microscope images of a 80 µm-square resin pattern containing 45 nm line and space (L&S) patterns surrounded by 1 µm line and space fringes, fabricated by UV nanoimprint (a) in air and (b) in PFP [10]. Non-uniformity is observable in the fine pattern region and bubbles are created in the surrounding fringes as shown in Fig. 2(a). In contrast, no anomalies were observed in the whole nanoimprint area for UV nanoimprint in PFP as shown in Fig. 2(b). Figure 2(c) shows a cross-sectional SEM image of the 45 nm line and space resin patterns [11]. The well-shaped patterns with 20-nm-thick residual layer were successfully fabricated by UV nanoimprint lithography using PFP. We can expect such patterns be uniformly fabricated in the entire area of the fine pattern region shown in Fig. 2(b), judging from their uniform visual qualities.

We have reported simulation studies on the resin filling process in UV nanoimprint lithography [12] based on continuum fluid dynamics taking surface tension into account by the use of contact angles at boundaries. We simulated the resin filling process under condensable gas ambient based on multi-phase fluidic flow systems [13].

The simulation model is shown in Fig. 3(a). When pressure is applied to the resin, the resin is filled into pattern cavities and stet gas is trapped in the cavity. The resin and the gas flows are solved simultaneously in a multi-phase flow system. The resin and the gas are assumed as incompressible and compressible Newtonian fluids, respectively. The Navier–Stokes equation and equation of continuity are numerically solved for liquid and gas phases based on the commercially available software U-FLOW/AG (Mizuho Information & Research Institute).

Table I shows typical parameters and feature sizes of the model structures for simulation. Figure 3(b) shows the simulation results of resin filling rate into the pattern cavity with various imprinting times for vacuum, air, and condensable gas ambient. In the air ambient,

bubbles are trapped and the template is stopped mid-way where the air pressure and press force are balanced. In the condensable gas ambient, the bubbles are eliminated and the resin is fully filled into the cavity. The resin filling time in condensable gas is almost the same as that in vacuum ambient. This result suggests that the condensable gas process is effective not only for bubble elimination but also for high-speed resin filling for practical use without the vacuum process.

During our JST-CREST project to study science and technology of UV nanoimprinting under a PFP atmosphere, we found several advantages and disadvantages of using PFP and commercially available UV-curable resin (PAK-01). The advantages are (i) viscosity reduction of the liquid resin [14], (ii) rapid filling of the liquid resin into mold cavities [8], (iii) reduction of demolding force on multiple detachments of the cured resin [15], and (iv)antifouling effect of resin adsorption to fluorinated silica molds [16]. The (i)-(ii) advantages are effective in high throughput in UV nanoimprinting, and the (iii)-(iv) advantages are effective in repeatability of UV nanoimprinting. By the contrast, the disadvantages are (v) large shrinkage of the UV-curable resin after curing by UV-exposure [17] and (vi) slightly degraded smoothness of the cured resin pattern edge [18]. Through the experiments, we were aware that the characteristics derived from PFP were explainable by absorption of PFP by the UV-curable resin.

SEM images of 45-nm L&S cured resin patterns were fabricated with a 90-nm-thick PAK-01 spin-coated film on a silicon wafer under an air atmosphere and a PFP atmosphere [10]. The fabrication of the fine resin patterns with a fluorinated silica mold with a depth of 90 nm made it clear that the smoothness of the resin pattern edge was degraded by the use of PFP. All of the resin convex lines were fabricated uniformly under a PFP atmosphere. The shapes of the line edge were undulated slightly. The mechanism due to absorption of PFP by the liquid UV-curable resin was recently clarified. We demonstrated a solution strategy [19]. The volume of uncured resin before UV-exposure increases due to the absorption of PFP, while the volume of cured resin after UV-exposure decreases due to the release of PFP.

To comprehend absorption of PFP by various UV-curable resins, we investigated the maximum values of PFP absorbed by commercially available UV-curable resins and acrylate type monomers causing radical photopolymerization [19]. The weights of the resins and monomers started to increase soon by exposure to a PFP atmosphere, with the viscosities decreased remarkably. The absorption of PFP depended clearly on chemical structures of the monomers. The following chemical structures of acrylate monomers selected for PFP absorption test were used: 1,6-hexanediol diacrylate **1**, tricyclodecanedimethanol diacrylate **2**, dipropenoic acid (1-methyl-1,2-ethanediyl) bis[oxy(2-hydroxy-3,1-propanediyl)] ester **3**, ditrimethylol propane tetraacrylate **4**, dipentaery thritol hexaacrylate **5**, 1-acryloxy-2-hydroxyl-3-methacryloxypropane **6**, 2,2,3,3,3-pentafluoropropyl acrylate **7**. Figure 4(a) shows the correlation of PFP molar absorption with Hildebrand's solubility parameter in terms of the monomers **1** – **7** and reference general chemicals **a** – **e**. The monomer **5** with a solubility parameter of 20 (J cm^{-3})$^{0.5}$ absorbed the most PFP. The monomer **7** was considered to absorb PFP readily because the monomer **7** has a pentafluoropropyl group. It was concluded that hydrocarbon chemicals without fluorine atoms and with a solubility parameter range of 18 – 22 (J cm^{-3})$^{0.5}$ absorbed a large amount of PFP. To investigate whether the shapes of cured resin patterns were affected by the absorption of PFP, two monomers, namely **1** and **3**, were selected for preparation of respective UV-curable resins. The resin-**1** comprises the monomer **1** [solubility parameter, 18.8 (J cm^{-3})$^{0.5}$] showing a large molar PFP absorption of 1.1 mol/mol (PFP dissolution, 0.69 g ml^{-1}), while the resin-**3** comprises the monomer **3** [solubility parameter, 23.5 (J cm^{-3})$^{0.5}$] showing a small molar PFP absorption of 0.5 (PFP dissolution, 0.20 g ml^{-1}). An increase in hydroxy group causes a solubility parameter of monomer to increase. The polar hydroxy group plays an important role in the size fidelity of UV-nanoimprinted resin patterns fabricated under a
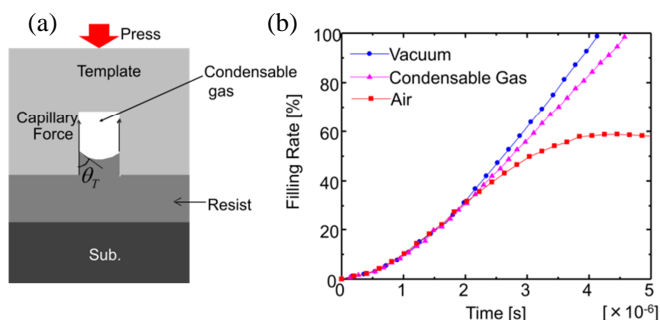
Figure 3. (a) Schematic of the simulation model. (b) Simulation results for resist filling rate into the pattern cavity with variation of imprinting times for vacuum, air, and condensable gas ambient.

PFP atmosphere. According to the results, a UV-curable resin comprising glycerol 1,3-diglycerolate diacrylate with three hydroxyl groups [solubility parameter, 26.0 (J cm^{-3})$^{0.5}$] was developed, which hardly absorbed PFP (PFP dissolution, 0.05 g ml^{-1}). It was possible to fabricate the 22-nm line-and-space cure resin patterns with the 30-nm-thick spin-coated film on a silicon wafer by UV nanoimprinting under a PFP atmosphere. As indicated in Fig. 4(b), the 22-nm convex resist lines showed the best line edge roughness value of LER (3σ) = 1.2 nm and the best line width roughness value of LWR (3σ) = 1.8 nm. The LER and LWR values satisfied values requested in 22 nm node NAND flash memories. The solution strategy to avoid influences of PFP on cured resin pattern is to use monomers except for a solubility parameter range of 18 – 22 (J cm^{-3})$^{0.5}$. The solubility parameter is a good index for designing high performance UV-curable resins suitable for UV nanoimprinting under a PFP atmosphere.

We aimed to execute more than 10,000 steps of UV nanoimprinting without significant imprint defects with a single mold. We focused on the condensable gas PFP, and a fluorosurfactant as an inner release agent [20]. As a means to improve the durability of the antisticking layer in the mold surface, a fluorosurfactant was tested.

PFP also has disadvantages such as the shrinkage of pattern height with respect to mold pattern depth caused by PFP absorption of the resin PAK-01 [17]. Kaneko et al. found that the degrees of PFP absorption by acrylic resins are dependent on their chemical structures, and that among acrylic monomers tested for PFP absorption, propylene glycol glycerolate diacrylate (Kyoeisha Chemical 70PA) [19], which is equivalent to the resin that composes C-TGC-02 (Toyo Gosei), showed the least PFP absorption. For this reason, C-TGC-02 was employed as the UV-curable resins. The pattern height loss of the acryl monomer 70PA owing to PFP absorption is estimated to be approximately 10% [19]. C-TGC-02 is a mixture of 93.1 wt% acryl resin 70PA, 4.9 wt% photoinitiator; 2-methyl-1[4-(methylthio) phenyl]-2-morpholinopropane-1-one (BASF Irgacure 907), and 2.0 wt% leveling agent for forming a uniform layer on a substrate. The chemical structure of the leveling agent is closed. The leveling agent is non-disclosure. This leveling agent may interact with an added fluorosurfactant. We therefore used C-TGC-02 without the leveling agent in this experiment.

The fluorosurfactant as an inner release agent used was F-444 (DIC). The fluorosurfactant does not participate in a polymerization reaction. Furthermore, C-TGC-02 and F-444 are dissolved with propylene glycol monomethyl ether (PGME). We added the fluorosurfactant to C-TGC-02 without the original leveling agent. The durability tests with the imprint pressured of 1.5 and 0.3 MPa using F-444 of 1pts were carried out. As a result, more than 20,000 steps of UV nanoimprinting were finally achieved with a single mold at 0.3MPa, as shown in Fig. 5.

In summary, UV nanoimprint is thought to be a promising nanofabrication technique and the use of condensable gas PFP provides some significant advantage in UV nanoimprint. Bubble defects disappear easily, and high throughput and reliable nanoimprint is attained. The process simulation in resin filling process under condensable gas ambient was demonstrated. The use of PFP occasionally results in undesirable side effects such as larger pattern shrinkage and rough pattern surface, but the side effects can be mitigated by appropriately selecting main component monomers with low PFP absorption. By using the synthetic UV resin of PFP low absorption developed here, the 22-nm convex resist lines showed the best value of LER(3σ) = 1.2 nm and the best value of LWR(3σ) = 1.8 nm, which are satisfied values requested in 22 nm node NAND flash memories. Furthermore, 20,000 repeated imprints with a single mold
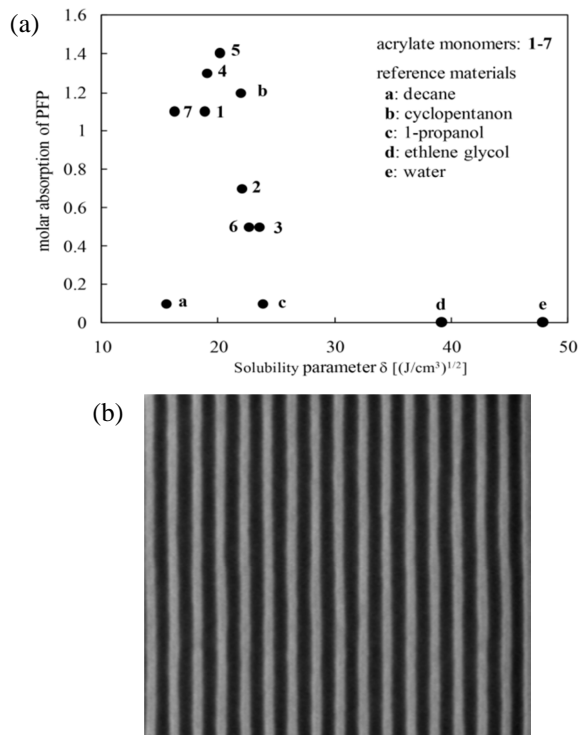
Figure 4. (a) Relationship of solubility parameter with molar absorption of PFP ion terms of acrylate monomers 1-7 and reference materials a-e. (b) CD-SEM image of 22-nm convex resist lines (line width: space width = 1:1) with the best line edge roughness value of LER (3σ) = 1.2 nm and the best line width roughness value of LWR (3σ) = 1.8 nm. (a) Schematic of the simulation model. (b) Simulation results for resist filling rate into the pattern cavity with variation of imprinting times for vacuum, air, and condensable gas ambient.
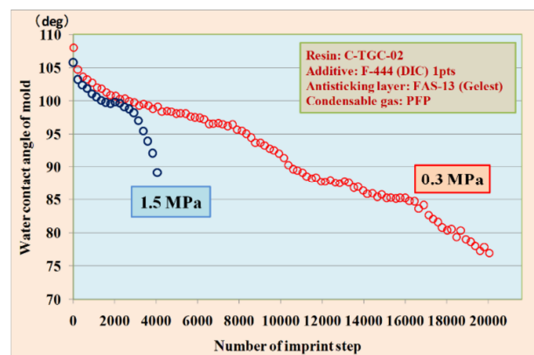
Figure 5. Water contact angle of mod versus number of imprint steps of resin with 1 pts F-444 surfactant at the pressures of 0.3 and 1.5 MPa.

were achieved by UV nanoimprint using surfactant-added UV resin and PFP atmosphere. From the above results, UV nanoimprint using PFP is so striking that we now think that use of PFP be an integral part of UV nanoimprint.

REFERENCES

[1] S. Y. Chou, P. R. Krauss, P. J. Renstrom, Imprint of sub-25 nm vias and trenches in polymers, *Appl. Phys. Lett.* **67**, 3114 (1995).

[2] J. Haisma, M. Verheijen, K. van den Heuvel, J. van den Berg, Mold-assisted nanolithography: A process for reliable pattern replication, *J. Vac. Sci. Technol. B* **14**, 4124–4128 (1996).

[3] H. Hiroshima, M. Komuro, N. Kasahara, Y. Kurashima, J. Taniguchi, Elimination of pattern defects of nanoimprint under atmospheric conditions, *Jpn. J. Appl. Phys.* **42**, 3849–3853 (2003).

[4] A. Fuch, M. Bender, U. Plachetka, U. Hermanns, H. Kurz, Ultraviolet-based nanoimprint at reduced environmental pressure, *J. Vac. Sci. Technol. B* **23**, 2925–2928 (2005).

[5] M. Colburn, S. Johnson, M. Stewart, S. Damle, B. J. Jin, T. Baiey, M. Wedlake, T. Michaelson, S. V. Sreenivasan, J. Ekerdt, C G. Willson, Step and flash imprint lithography: An alternative approach to high resolution patterning, *Proc. SPIE* **3676**, 379–389 (1999).

[6] S. Reddy, R. T. Bonnecaze, Simulation of fluid flow in the step and flash imprint lithography process, *Microelect. Eng.* **82**, 60 –70 (2005).

[7] H. Hiroshima, M. Komuro, Control of bubble defects in UV nanoimprint, *Jpn. J. Appl. Phys.* **46**, 6391–6394 (2007).

[8] H. Hiroshima, M. Komuro, UV-nanoimprint with the assistance of gas condensation at atmospheric environmental pressure, *J. Vac. Sci. Technol. B* **25**, 2333–2336 (2007).

[9] H. Hiroshima, Quick cavity filling in UV nanoimprint using pentafluoropropane, *Jpn. J. Appl. Phys.* **47**, 5151–5155 (2008).

[10] H. Hiroshima, Q. Wang, S.-W. Youn, 45 nm hp line/space patterning into a thin spin coat film by UV nanoimprint based on condensation, *J. Vac. Sci. Technol. B* **28**, C6M12 (2010).

[11] H. Hiroshima, K. Suzuki, Throughput of ultraviolet nanoimprint in pentafluoropropane using spin soat films under thin residual layer conditions, *Jpn. J. Appl. Phys.* **51**, 06FJ10 (2012).

[12] D. Morihara, Y. Nagaoka, H. Hiroshima, Y. Hirai, Numerical study on bubble trapping in UV nanoimprint lithography, *J. Vac. Sci. Technol. B* **27**, 2866 –2868 (2009).

[13] Y. Nagaoka, R. Suzuki, H. Hiroshima, N. Nishikura, H. Kawata, N. Yamazaki, T. Iwasaki, Y. Hirai, Simulation of resist filling properties under condensable gas ambient in ultraviolet nanoimprint lithography, *Jpn. J. Appl. Phys.* **51**, 06FJ07 (2012).

[14] H. Hiroshima, H. Atobe, Q. Wang, Viscosity of a thin film of UV curable resin in pentafluoropropane, *J. Photopolym. Sci. Technol.* **23**, 45 (2009).

[15] H. Hiroshima, Release force reduction in UV nanoimprint by mold orientation control and by gas environment, *J. Vac. Sci. Technol. B* **27**, 2862–2865 (2009).

[16] K. Kobayashi, S. Kubo, H. Hiroshima, S. Matsui, M. Nakagawa, Fluorescent microscopy proving resin adhesion to a fluorinated mold surface suppressed by pentafluoropropane in step-and-repeat ultraviolet nanoimprinting, *Jpn. J. Appl. Phys.* **50**, 06GK02 (2011).

[17] Q. Wang, H. Hiroshima, Effects of environmental gas in UV nanoimprint on the characteristics of UV-curable resin, *Jpn. J. Appl. Phys.* **49**, 06GL04 (2010).

[18] Q. Wang, H. Hiroshima, K. Suzuki, S.-W. Youn, *In-situ* evaluation of air/oxygen percentage variation by introducing 1,1,1,3,3-pentafluoropropane in ultraviolet nanoimprint lithography, *Jpn. J. Appl. Phys.* **51**, 118002 (2012).

[19] S. Kaneko, K. kobayashi, Y. Tsukidate, H. Hiroshima, S. Matsui, M. Nakagawa, Morphological changes in ultraviolet-nanoimprinted resin patterns caused by ultraviolet-curable resins absorbing pentafluoropropane, *Jpn. J. Appl. Phys.* **51**, 06FJ05 (2012).

[20] S. Iyoshi, M. Okada, T. Katase, K. Tone, K. Kobayashi, S. Kaneko, Y. Haruyama, M.Nakagawa, H. Shiroshima, S. Matsui, Study of demolding characteristics in step-and-repeat ultraviolet nanoimprinting, *Jpn. J. Appl. Phys.* **52**, 06GJ04 (2013).